



ORIGINAL ARTICLE

Flexural Strength of Concrete Beam Reinforced with Basalt Fiber Reinforced Polymer and Steel Bars

Joseph Toh Sheng Ngu, *Mazizah Ezdiani Mohamad, and Teck Sung Sie

Centre of Research for Innovation and Sustainable Development (CRISD), School of Engineering and Technology, University of Technology Sarawak, 96000 Sibul, Sarawak, Malaysia

ABSTRACT - In this paper, the flexural behavior of concrete beams reinforced with basalt fibre reinforced polymer (BFRP) bars is compared with concrete beams reinforced with steel bars. A total of six beams, each consisting of three BFRP reinforced concrete (RC) beams and steel-RC beams with various reinforcement ratio of 0.5%, 1.0% and 2.0%, were tested to failure under a four-point load with dimensions of 150 mm × 300 mm × 1700 mm at compressive strength of 51.3 N/mm². The cracking behavior, failure modes, and load-deflection behavior of the beams were investigated. The results show that increasing the reinforcement ratio effectively restrains the crack widths and deflections while increasing the flexural capacity of the beams. The test results showed that the increase in the reinforcement ratio improved the flexural capacity of the BFRP-RC beams similarly to steel-RC beams. Moreover, the concrete beams with steel bars as reinforcement recorded slightly higher flexural capacity than that of BFRP bars as reinforcement.

ARTICLE HISTORY

Received: 9 Nov 2022

Revised: 16 Dec 2022

Accepted: 15 Jan 2022

KEYWORDS

Reinforced concrete, BFRP bars, Flexural performance, Reinforcement ratio, Crack pattern

INTRODUCTION

Civil engineers have made great efforts to improve the behavior of concrete structures, shear strength, flexural strength, ductility, elastic modulus, compressive strength, and other properties by adding steel reinforcement. Steel reinforcement has good strength and ductility but it will suffer from corrosion when exposed to an open environment.

In addition, Malaysia is a tropical country with relatively high humidity. The average annual humidity is within the range of 74% to 84% [1],[2]. This contributes to the higher occurrence of steel corrosion in reinforced concrete, leading to structural defects. At the same time, it shortens the service life of the concrete structure.

To overcome these deficiencies, the BFRP bar is an alternative solution to replace conventional steel bars as reinforcement for RC structural due to its non-corrosive characteristic. Meanwhile, without the deterioration of reinforcement, it increases the life span of the concrete structures.

Furthermore, many studies have been conducted on fibre-reinforced polymer (FRP) reinforced concrete, with much of the research focused on the applications of Carbon-FRP and Glass-FRP rebars. FRP rebar has demonstrated successful application for both flexural and shear reinforcement in various reinforced concrete structural elements including RC beams [3],[4]. However, little research has been conducted on BFRP to understand how it complements the advantages of an FRP system.

Hence, the static response, behavior of RC beam reinforced with BFRP bars, and previous experimental testing was explained and summarized in this paper. The experimental results were predicted by ACI 440.1R-15 equations [5]. The ACI equation indicated that the flexural strength was directly related to the reinforcement ratio regardless of the failure mode.

*Corresponding Author: Mazizah Ezdiani Mohamad. University of Technology Sarawak (UTS), email: mazizah@uts.edu.my

METHOD STATEMENT

This paper provides relevant code of practices, strength and performance of BFRP concrete beam, flexural crack pattern, and reinforcement ratio through literature studies. The experimental data of researchers are reported and discussed. Subsequently, review the parameter that influences the load-carrying capacity and flexural strength. The results are used to evaluate the efficiency of BFRP bars as internal reinforcement for reinforced concrete beams.

PREVIOUS STUDY ON BFRP CONCRETE BEAM

Literature studies have been carried out to evaluate the behavior and performance of the BFRP concrete beam. The different parameters used to fabricate the test specimens will generate different responses and performances. Therefore, it is significant to gain a better understanding of the feasibility of fabricating the test specimens. Also, the predicted response and behaviour of the BFRP RC beam can reliably resemble reality. According to Fared *et al*, [6], the flexural capacity of BRP reinforced beam was significantly affected by the type and reinforcement ratio (ρ). The increasing trend of the flexural capacity for BFRP-RC beams with increasing ρ agrees well with the ACI 440.1R-15 [5] moment equation for the compression-controlled failure mode.

The research studies are focused on experimental studies on the BFRP RC beam. Experimental approaches offer researchers a more promising way to estimate accurate causes and effects. Besides, experimental studies can be referred to as guidance and comparison for future works.

Furthermore, most of the researchers were using the four-point load bending test method to investigate the flexural behavior of the concrete beams. In four-point bend tests, the maximum flexural stress is spread over the section of the beam between loading points. The stress concentration of a four-point test is over a larger region, avoiding premature failure [7]. In three-point load, the stress is more concentrated under the injected loading [8]. The typical crack failure is vertical to the loading. Also, a three-point test best applies where the material is homogeneous, such as plastic materials [8],[9]. A four-point test tends to be the best choice if the material is not homogeneous, such as composites [7],[10].

Apart from that, the behavior of the crack propagation in the tested beams is flexural-cracking patterns. The first cracks always appeared in the pure bending region of the beams. The crack starts from the bottom surface of the beam and propagate vertically toward the compression zone. As the load increases, more cracks will appear outside the pure bending region towards the supports. On the other hand, different scales of the RC beam will affect the failure mode. The summary of the failure mode from the different authors included:

- a) Cracking occurred at the location of the basalt reinforcement and extended along the length of the beam. The slippage was identified by the formation of cavities, located directly behind the reinforcing bars [11].
- b) There was no rupture or slippage of basalt bars in the flexural reinforcement. The failure of the beam was due to shear force in the support zones [12].
- c) Rupture of BFRP bars and the failure mode due to the shear cracks [13].
- d) Longitudinal cracks at the level of the reinforcement appeared between two cracks. This phenomenon is due to slippage between the reinforcement bars and surrounding concrete. The beam fails in concrete crushing [14].
- e) Beams with BFRP stirrups all failed in shear by stirrups rupture. The concrete in the compression zone of the shear crack was crushed [15].
- f) Flexural cracks developed throughout the beam length [16],[17],[18]. The concrete in the compression zone was crushed in the constant moment region [18].

Moreover, to minimize the confining effect of the shear reinforcement on the flexural behavior, no stirrups were used in the constant moment zone [10]. The test specimens were designed to fail by concrete crushing in the constant moment zone.

METHOD AND EXPERIMENTAL SETUP

Three BFRP-RC beams and three Steel-RC beams were fabricated in the size of 1700 mm (L) × 150 mm (W) × 300 mm (H). The concrete cover was 25 mm. The design characteristic concrete compressive strength is 50 MPa, and the BFRP and steel longitudinal reinforcement ratio ($\rho_f = 1.0\%$, 1.5% , and 2.2%). The shear reinforcement omitted at the moment region to omit the factor that affects the flexural behaviour. Figure 1 shows the detailing of the BFRP and Steel-reinforced concrete beam.

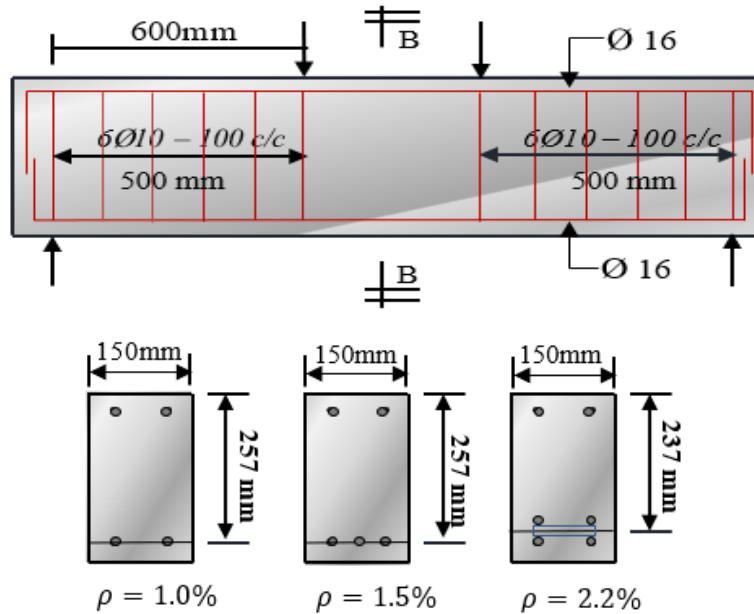


Figure 1. Detailing of Reinforced Concrete Beam

The beam specimens were tested under two load cases, namely flexural loads. The beam specimens will support by steel roller and rocker at the ends and subjected to two-point loads. The distance between the two-point loads is 300 mm for flexural tests. The typical setup is shown in Figure 2.

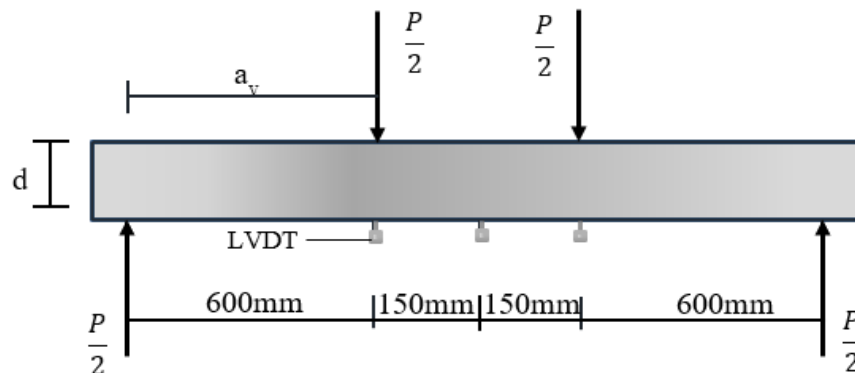


Figure 2. Flexural Load Test

The load was applied to the beam using a static actuator system (500 kN), a distribution beam, and some roller and rocker systems. The distribution beam transforms the load induced by the actuator into two-point loads acting onto the beam specimen through the roller and rocker system.

Three Linear Variable Differential Transducers (LVDT) (Brand: TML, stroke: 50-100 mm) was placed under the beam spacing at the mid-span and below the point loads to measure the vertical displacements developed at the region, as demonstrated in Figure 2. These LVDT devices were connected to a data logger (Brand: TML, model: TDS-530) for data acquisition. All the measuring devices were ensured to be calibrated, and before the commencement of the test, the readings were set to initial (zero). The data obtained was monitored using a computer during the testing. The accuracy of equipment is tabulated in Table 1.

Table 1. Accuracy of Equipment

Equipment / instrument	Brand/ Model	Description	Data accuracy
Actuator	661.23 F-01	Capacity 500kN	± 0.1 kN
LVDT	CDP-100	Stroke 50 and 100 mm	± 0.01 mm
Data logger	TML TDS-530	50 Channels	0.1s measurement speed

TEST PROCEDURE

The flexural load tests were carried out in the laboratory. The sequence of loading followed the standard procedures recommended by the ASTM D6272-17 [19] standard.

The experiment started with a load-controlled mode at the elastic stage and was followed by the displacement-controlled mode during the yielding stage. The purpose of changing the load-controlled mode to the displacement-controlled mode was to obtain a smooth load-displacement curve. The reading was taken at a rate of every 5% of the estimated load increment or every 0.5 mm of the beam displacement, whichever achieves first. The load was maintained for at least 1 minute before the data logger recorded the readings.

During the testing, the propagation of the crack with respect to the load applied was monitored. The load-displacement response of the beam was monitored by using a computer. The test process stops as the beam failed.

FLEXURAL STRENGTH

In reinforced concrete design, the nominal flexural strength of an FRP-RC structure can be predicted based on stress-strain, internal force equilibrium, and the strength limits state. The strength limit states are important in determining the concrete member whether the flexural strength is controlled by concrete crushing or FRP rupture [20]. Theoretically, when the strength of reinforcement is fully utilized, the concrete member is considered to be under-reinforced (FRP rupture) and the effectiveness of flexural reinforcement is reduced when the cross-section becomes over-reinforced (concrete crushing) [3].

The above-mentioned failure mode is dependent on the reinforcement ratio (ρ_f) and balanced reinforcement ratio (ρ_{fb}). If the reinforcement ratio is less than the balanced ratio ($\rho_f < \rho_{fb}$), the failure mode is governed by FRP rupture. Otherwise, ($\rho_f > \rho_{fb}$) the failure mode is governed by concrete crushing. Based on ACI 440.1R-15 [3], the reinforcement ratio can be calculated using Eq.1 and the balanced ratio can be calculated using Eq. 2.

$$\rho_f = \frac{A_f}{bd} \quad (1)$$

Where: A_f = the area of fibre-reinforced polymer (FRP) reinforcement, b = the area of tension steel reinforcement, d = the distance from extreme compression fiber to centroid of tension reinforcement

$$\rho_{fb} = 0.85\beta_1 \frac{f'_c}{f_y} \left(\frac{87000}{87000+f_y} \right) \quad (2)$$

Where: β_1 = the factor taken as 0.85 for concrete strength f'_c up to and including 28 MPa. For strength above 28 MPa, this factor is reduced continuously at a rate of 0.05 per each 7 MPa of strength over 28 MPa but is not taken less than 0.65, f'_c = the specified compressive strength of concrete. f_y = the specified yield stress of non-prestressed steel reinforcement.

Furthermore, in the tension-controlled region, using higher concrete compressive strengths is not necessarily cost-effective because the section will achieve the same moment capacity as an equally sized and reinforced section using lower concrete compressive strength [21]. Therefore, Eq. 3 and Eq. 4 are important to determine the moment in reinforced concrete design to provide an optimum reinforcement ratio. When the FRP reinforcement ratio, ρ_f , is higher than ρ_{fb} , flexural failure is expected to occur due to concrete crushing, and vice versa. The equation for nominal flexural strength is according to ACI440.1R-15 [3].

Concrete Crush,

$$M_n = \rho_f f_f \left(1 - 0.59 \frac{\rho_f f_f}{f'_c} \right) b d^2 \quad (3)$$

Where: ρ_f = fibre-reinforced polymer reinforcement ratio, f_f = stress in FRP reinforcement in tension, f'_c = specified compressive strength of concrete, b = the area of tension steel reinforcement, d = the distance from extreme compression fiber to centroid of tension reinforcement

FRP Rupture,

$$M_n = A_f f_{fu} \left(d - \frac{\beta_1 c}{2} \right) \quad (4)$$

Where: f_{fu} = the design tensile strength of FRP, defined as the guaranteed tensile strength multiplied by the environmental reduction factor, C is the distance from extreme compression fibre to the neutral axis at balanced strain condition, β_1 = the factor is taken as 0.85 for concrete strength f'_c up to and including 28 MPa.

The theoretical flexural capacity for Steel-RC beam is computed from ACI 318R-11 [22]. The moment in reinforced concrete design can calculate using Eq. 5 and Eq. 6.

Concrete Crush,

$$M_n = \phi \rho f_y b d^2 \left(1 - \frac{1}{1.7} \rho \frac{f_y}{f'_c} \right) \quad (5)$$

Where: ϕ = strength reduction factor, f_y = specified yield stress of non-prestressed steel reinforcement, ρ = reinforcement ratio, f'_c = specified compressive strength of concrete, b = the area of tension steel reinforcement, d = effective depth of specimen

Steel Rupture,

$$M_n = A_s f_y \left(d - \frac{a}{2} \right) \quad (6)$$

Where: A_s = area of longitudinal tension reinforcement, a = depth of equivalent rectangular stress block, f_y = specified yield stress of non-prestressed steel reinforcement, d = effective depth of specimen.

Table 2 showed that the experimental moment is slightly lower compared to ACI design code prediction. In design code prediction, increasing the reinforcement ratio were shown to be effective in increasing the moment capacity. The BFRP-RC beam reinforcement ratio, ρ_f increased from 1.04 % to 1.56 % did not show a significant in increase the ultimate moment capacity. Beam BF8 increased flexural capacity by 2.77 % compared to BF7. Meanwhile, the beam BF9 increased flexural capacity by 37.78 % compared to BF7.

Similarly, flexural capacity for Steel-RC beam increased as reinforcement ratio increased. Beam SF6 increased flexural capacity by 30.69 % and 15.41 and compared to SF4 and SF5, respectively. Besides, compared BF9 and SF6 with same reinforcement ratio and concrete compressive strength, it noticed that the BF9 reduced 28.48 % in flexural capacity. This phenomenon may cause by the reduction of flexural resistance in BFRP stirrup especially around the bending portion. This has been reported by ACI 440.1R [3] which the reinforcement is calculated as smaller as $0.004 E_f$ or $0.4 f_{Fu}$ to avoid failure at the bend portion of the FRP stirrup.

In addition, the higher reinforcement ratio showed higher post-cracking bending stiffness and experienced flexural-critical failure under static loading. Hence, higher reinforcement ratios exhibited improved patterns characterized by better distribution and smaller crack widths. Apart from that, the flexural strength affected by the neutral-axis depth. The increase of reinforcement ratio will reduce the neutral-axis depth. This led to increase the compression area. The equilibrium of forces required a larger compression block to increase the stiffness of the beams.

The experimental load carrying capacity and flexural strength can be calculated using Eq. 7 and Eq. 8, respectively. The load carrying capacity and flexural strength is computed in Table 2. The calculation step can be derived from shear and moment diagram, Figure 3. The acceptable of the reliability ratio of the result obtained should be within the range of 0.90 to 1.10.

Shear Force,

$$V(x) = \frac{1}{2} F \quad (7)$$

Where: F = Concentrated Load

Bending Moment,

$$M(x) = \frac{1}{2} F x \quad (8)$$

Where: F = concentrated load, x = length of span in direction from concentrated load to centroid of support

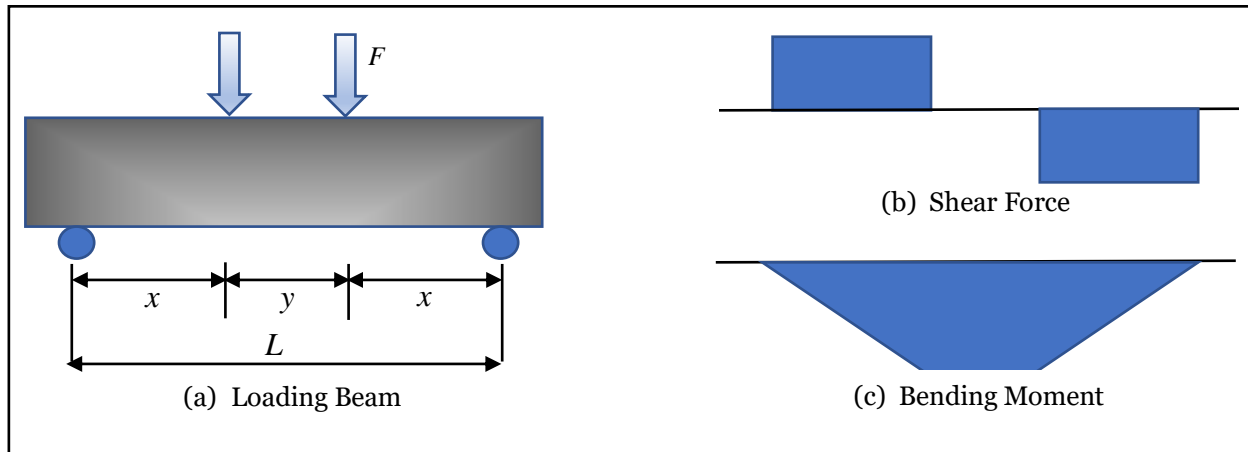

Figure 3. Shear Force and Bending Moment Diagrams

Table 2. Load Carrying Capacity and Flexural Strength

Testing Specimens	Compressive Strength, N/mm^2	Reinforcement Ratio, ρ_f	Load Carrying Capacity, kN	Experimental Moment, M_{exp} (kN.m)	ACI Moment, M_{ACI} (kN.m)	$\frac{M_{exp}}{M_{ACI}}$
BF7	51.3	1.04	132.71	46.45	59.20	0.78
BF8		1.56	136.39	47.74	69.47	0.69
BF9		2.27	182.85	64.00	67.59	0.95
SF4		1.04	179.75	89.88	54.62	1.65
SF5		1.56	203.56	101.78	78.95	1.29
SF6		2.27	234.92	117.46	91.95	1.28

LOAD DEFLECTION

The load-displacement relationship presents the behavior of a specimen with important information such as stiffness, yield point, load capacity, and ductility. Figure 4, and 5 shows the experimental load-deflection graphs for the reinforced beams under static. The curves presented illustrate the mid-span deflection results obtained from the linear variable differential transformer (LVDT). Figure 4, illustrated the behavior of the BFRP-RC beam under static load. BFRP-RC beam displayed a bi-linear relationship up to total failure and the beam specimen exhibited pre-crack and post-crack responses. The elastic behavior of each graph was representative of the pre-cracking stage of the RC beam. In this stage, the induced stress mostly is absorbed by the reinforcement bar and assume the concrete beam does not carry any tension. Subsequently, the incremental load causes the cracking occurs when the maximum service load moment exceeds the cracking moment. Referring to Figure 4, the RC beams shown the characteristic of post-cracking response. The load decreases after the initial peak and then begins to increase again. After cracking, the stiffness increased linearly until total failure caused by critical flexural crack.

Furthermore, Figure 5 shows the applied load versus the average mid-span deflection responses. BFRP and Steel-RC beam displayed similar behavior in which the curve is bi-linear up to total failure. The first linear portion of each graph was representative of the uncracked section. Owing to the lower flexural stiffness of the BFRP bars compared to steel, the BFRP-RC beams had lower stiffness compared to Steel-RC beams.

The stiffness reduction can be observed in the load-deflection curves as a small discontinuity and the subsequent reduction in the slope of the load-deflection curve. The reduction of stiffness for BFRP-RC beams under flexural load were 36.33 kN in average. Meanwhile, reduction stiffness for Steel-RC Beams

under flexural were 56.33 kN in average. Comparing the deflection between BFRP and Steel-RC beam the larger deflection in the order of 1.75 to 2.0 times the deflection of the Steel-RC beam. Among the BFRP-RC beam tested under flexural load, beam BS9 exhibited the lowest post-cracking stiffness until failure at ultimate load of 182.85 kN and 19.52 mm mid span deflection. Compared to SF6 with same reinforcement ratio and concrete strength, the beam failure at ultimate load of 234.92 kN and 15.67 mm. Obviously, BFRP-RC beam had higher crack width compared to Steel-RC beam. This is due to the lower modulus of elasticity and the bond characteristics of the BFRP bar.

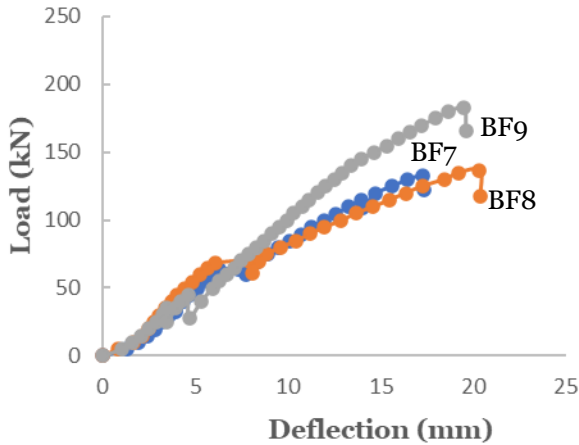


Figure 4. Load-Deflection Response of Flexural BFRP-RC Beams

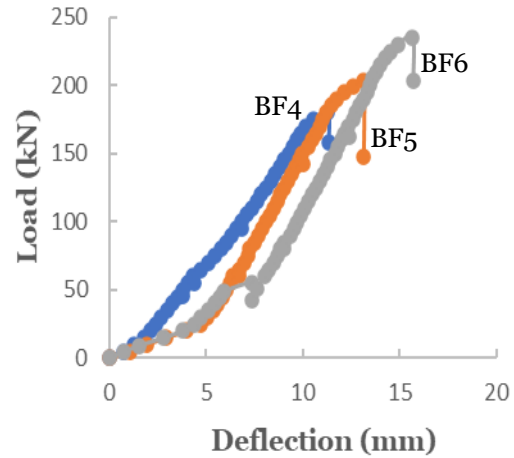


Figure 5. Load-Deflection Response of Flexural Steel-RC Beam

FLEXURAL BEHAVIOR AND FAILURE MODE

The BFRP and Steel-RC beams were designed as over-reinforced which the concrete beams failed by concrete crushing when the concrete reached its maximum compressive strain of $\epsilon_{cu} = 0.0030$ and 0.0035 according to ACI 440.1R-15 [3].

The stresses in a typical cross-section of a reinforced concrete beam for flexural tests are longitudinal stresses. When the beam specimens were subjected to bending, transverse tensile cracks will occur when the tensile strength of the concrete is reached.

The BFRP-RC beam specimens had similar behavior under flexural loading. Initially, the solid beam was in elastic state. The beam was able to sustain load over a very small deflection prior to cracking. The first sign of flexural cracking occurred around the mid-span and in the constant moment region between two-point loads. The first crack load ranged from 28 kN to 71 kN with average of 36 kN, Figure 6.

After the first crack occurred, the rigidity of every specimen decreased. As the load gradually increased, flexural cracks began to propagate towards the supports at compressive zone. Observations from Figure 6, BFRP-RC beams had similar general behavior and cracking pattern. Two major cracks propagated throughout the height of the beam. Widening of existing cracks occurred, especially around the mid-span. This can lead consideration of prior warning of the beam specimen failure.

Figure shows two major cracks were vertical extended to compressive zone and propagated horizontal. This indicated the critical failure of the specimens fail by concrete crushing. The experiment was stopped before both of the horizontal crack connected to prevent catastrophic failure of the beam specimen.

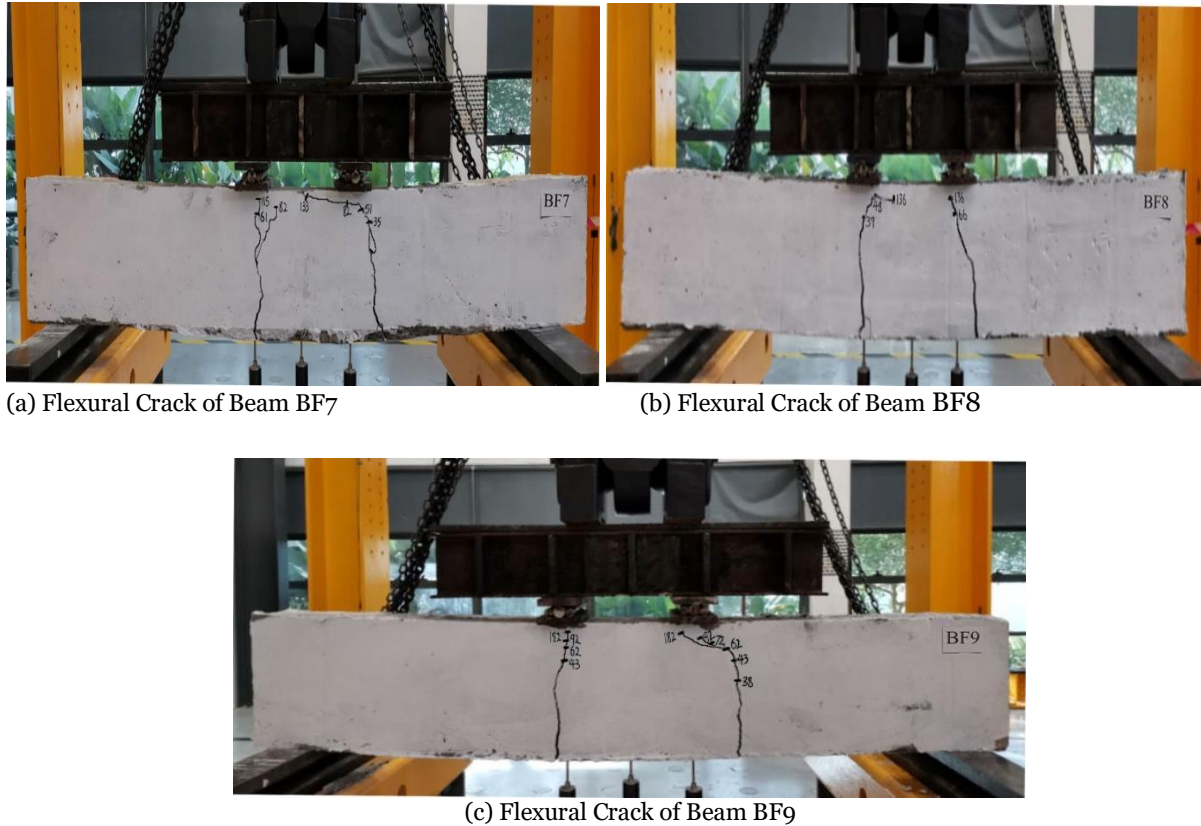
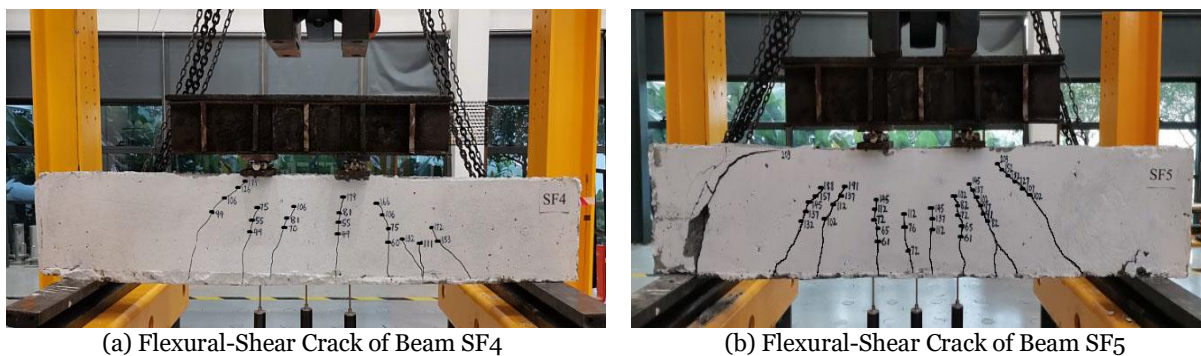
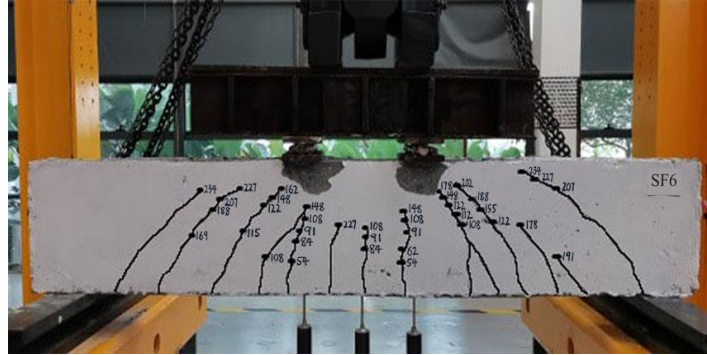


Figure 6. Failure Mode of BFRP-RC Beam Under Flexural Load

In contrast to BFRP-RC beams, the signs of flexural-shear were observed for Steel-RC beams. The behavior of Steel-RC beam showed initial signs of vertical flexural cracks within the pure flexure region. These initial cracks continued to expand and propagate vertically, closer towards the loading. As the load increased, additional cracks developed throughout the span of the beam which closer to the supports. The crack developed along the span were quite consistent with average crack spacing of 120 mm.

These phenomena caused by the stress distributed from the mid span throughout to the supports. This led to the concentration of high stress near the supports which resulted the diagonal crack in the beam. Hence, the critical shear cracks resulted in the rupture of the reinforcement bar, accompanied by popping noises. The critical diagonal crack failure was indicated in Figure 7.





(c) Flexural-Shear Crack of Beam SF6

Figure 7. Failure Mode of Steel-RC Beam Under Flexural Load

CONCLUSION

The data and results for a total of six (6) reinforced concrete beams under static loading have been discussed. The following are the main conclusions of the study:

1. BFRP bars tend to be brittle, with little or no ductility. BFRP bars are low elastic modulus and non-yield characteristics.
2. The flexural load for the BFRP beams were reduced compared to the reference beam or control beam.
3. The ratio of the beam reinforcement to the calculated balanced reinforcement (ρ_f/ρ_{fb}) can be used as an indicator for the failure mode of the BFRP RC beams. Concrete crushing on the top surface occurred for BFRP RC beams reinforced with more than the balanced reinforcement.
4. The reinforcement ratios affect flexural strength and load-carrying capacities. The concrete is important for the transmission of the strain to reinforcement bars.
5. The failure mode for all BFRP-RC beams were flexural failure. Vice versa, the failure mode for Steel-RC beams were flexural-shear failure.
6. The BFRP-RC beams showed typical bilinear behavior for strain and deflection until failure. The pre-cracking response and cracking loads of all the beams were nearly unaffected by the reinforcement ratio, since they are governed by the gross concrete section. After the beams crack, the increase in stiffness or reduction in reinforcement strains was proportional to the reinforcement ratio.
7. Omitted the stirrup at the moment region to omit the effect of the factor on flexural behaviour.
8. The acceptable of the reliability ratio of the result showed that the ACI 440.1R-15 [3] design for concrete beams reinforced with BFRP bars were over predicted in term of the moment carrying capacity.

ACKNOWLEDGMENT

The authors are grateful to the University of Technology Sarawak (UTS) research fund of Project ID: UCTS/RESEARCH/<1/2019/09>(01).

REFERENCES

- [1] Jamaludin, N. & Izma, N., "Thermal Comfort of Residential Building in Malaysia at Different Micro-Climates." *Procedia - Social and Behavioral Sciences*, 170, pp.613–623, 2015.
- [2] M Syafiq Syazwan Mustafa1, Fatimah Yusop, M D Amir Abdullah, M A A Rahman, Kamarul Aini Mohd Sari1, Fahmi A R, Mohd Arif Rosli, Norshuhaila Mohamed Sunar, and Azian Hariri. "Humidity control strategies in operation theatre Malaysia." *IOP Conf. Series: Earth and Environmental Science* 373, 012016, 2019.

- [3] M.S. Alam, A. Hussein, “Experimental investigation on the effect of longitudinal reinforcement on shear strength of fibre reinforced polymer reinforced concrete beams,” *Can. J. Civ. Eng.* 38 (3) 243–251, 2011.
- [4] A.F. Ashour, Flexural and shear capacities of concrete beams reinforced with GFRP bars, *Constr. Build. Mater.* 20 (10) 1005–1015., 2005.
- [5] American Concrete Institute (ACI) Committee 440. “Guide for the Design and Construction of Structural Concrete Reinforced with Fiber-Reinforced Polymer (FRP) Bars”. American Concrete Institute, ACI 440.1R-15, Farmington Hills, Michigan, USA, 2015.
- [6] Farid Abed, Mustafa Al-Mimar, Sara Ahmed, “Performance of BFRP RC beams using high strength concrete,” *Composites Part C: Open Access*, Volume 4, 100107, ISSN 2666-6820, 2021.
- [7] Podstawka, A. et al. “Analytical and Statistical Evaluation of FRC Bending Tests Layouts”, *Advanced Materials Research*, 1106, pp. 118–121., 2015.
- [8] Nandhini, M.S. & Malarvizhi, M.S., “Hybrid Reinforced Concrete Beam Using Steel and BFRP Bars.”, 2017.
- [9] Azzam, A. and Li, W. “An experimental investigation on the three-point bending behavior of composite laminate”, *IOP Conference Series: Materials Science and Engineering*, 62(1), 2014.
- [10] Hammant, B. “The use of 4-point loading tests to determine mechanical properties”, *Composites*, 2(4), pp. 246–249, 1971.
- [11] Gohnert, M., Van Gool, R. & Benjamin, M. “BFRP reinforced in concrete beams in flexure”, *The Structural Engineer*, pp. 38-43, 2014.
- [12] Urbanski, M., Lapko, A. & Garbacz, A. “Investigation on Concrete Beams Reinforced with Basalt Rebars as an Effective Alternative of Conventional R / C Structures Investigation on Concrete Beams Reinforced with Basalt Rebars as an Effective Alternative of Conventional R / C Structures.” *Procedia Engineering*, 57, pp.1183–1191, 2016.
- [13] Rudžinskis, E., “Flexural behaviour of BFRP rebar reinforced concrete beams,” 10(2), pp.134–170, 2017.
- [14] Elgabbas, F. et al., “Experimental testing of basalt-fiber-reinforced polymer bars in concrete beams.” *Composites Part B*, 91, pp.205–218, 2016.
- [15] Tomlinson, D., and Fam, A. “Performance of Concrete Beams Reinforced with Basalt FRP for Flexure and Shear.” *ASCE Journal of Composites for Construction*, 19 (2), 1–10, 2015.
- [16] Sunny, J.C. et al., “Experimental study on properties of concrete reinforced with basalt bars.” pp.1524–1529. *Transportation Research Board of National Academies*, Project No. 86, 2016.
- [17] Ovitigala, T. “Structural Behavior of Concrete Beams Reinforced with Basalt Fiber Reinforced Polymer (BFRP) Bars.” PhD Thesis, University of Illinois, Chicago, 2012.
- [18] Adhikari, S. “Mechanical Properties and Flexural Applications of Basalt Fiber Reinforced Polymer (BFRP) Bars.” MSc Thesis, Department of Civil Engineering, University of Akron, Ohio, USA, 2009.
- [19] ASTM D6272-17 (2017), Standard Test Method for Flexural Properties of Unreinforced and Reinforced Plastics and Electrical Insulating Materials by Four-Point Bending, ASTM International, West Conshohocken, PA.
- [20] Koyzis, D.T. et al., (2016). Behaviour of concrete beams reinforced with GFRP bars under static & impact loading. *Thesis*, 19(1), p.484.
- [21] International Federation for Structural Concrete (FIB). (2007). “FRP Reinforcement in RC Structures.” *fib Task-Group 9.3*, 2007, *fib Bulletin* 40, pp 1-147.
- [22] ACI Committee 318. (2011). “Building Code Requirements for Structural Concrete (ACI 318-11) and Commentary (ACI 318R-11).” ACI, Farmington Hills, Michigan, USA.